Sampling conditions of the 3D fan beam X ray transform

L. Desbat, S. Roux
TIMC-IMAG, UMR CNRS 5525,
IAB, faculté de Médecine, UJF
38706 La Tronche France,
Laurent.Desbat@imag.fr

P. Grangeat, A. Koenig
LETI, CEA-DRT,
17 rue des Martyrs,
38054 Grenoble, France

Abstract

We give the sampling conditions of the 3D fan beam X ray transform (3DFBXRT). The motivation of this work lie in the fact that helical tomography with a single detector line is simply a sampling of this transform under the helical constraint. We give a precise description of the geometry of the essential support of Fourier transform of the 3DFBXRT and we show how to derive efficient sampling.

1 Introduction and notation

1.1 Helical tomography, 3DFBXRT, 3DPXRT

We first show that helical tomography is directly related to the 3D fan beam X ray transform (3DFBXRT). Indeed, let f be the (smooth) 3D attenuated function measured in a scanner of radius $r > 0$, we define the 3DFBXRT perpendicular to $e_3 = (0, 0, 1)^t$ (scanner rotation axis) by:

$$g(\beta, \alpha, t) = \mathcal{D}_{e_3{}^\perp} f(\beta, \alpha, t) = \int_{L_{\beta,\alpha,t}} f(x)dx, \tag{1}$$

where $x \in \mathbb{R}^3$, $L_{\beta,\alpha,t}$ is the line in the plane perpendicular to e_3 at abscisse t ($t \in \mathbb{R}$), joining the source placed at $r(\cos\beta, \sin\beta, 0) + te_3$, $\beta \in [0, 2\pi[$ and the detector with position angle $\alpha \in [0, \pi[$, see figures 1 and 2. Clearly, helical tomography with a single detector line is a sampling of $\mathcal{D}_{e_3{}^\perp} f$ under the helical constraint, i.e., with t and β linearly dependent $t(\beta) = (2\pi/T)\beta$, T being the pitch. Usually t is along the scanner axis. In dynamic tomography, i.e., when measuring a slice of a moving organ, t is the time (dynamic tomography is just helical tomography along the time axis).

The 3DFBXRT is linked to the 3D Parallel XRT (3DPXRT) defined by

$$\mathcal{P}f(\phi, s, t) = \int_{\mathbb{R}} f(s\theta(\phi) + u\zeta(\phi) + te_3)du, \tag{2}$$

where $\zeta(\phi) = (\sin\phi, \cos\phi, 0)^t$, $\theta(\phi) = (\cos\phi, \sin\phi, 0)^t$, $\phi \in [0, 2\pi[$, $(s, t) \in \mathbb{R}^2$. Indeed,

$$\mathcal{D}_{e_3{}^\perp} f(\beta, \alpha, t) = \mathcal{P}f(\beta + \alpha - \pi/2, r\sin\alpha, t). \tag{3}$$

As we have shown in [12], efficient sampling in parallel helical tomography can be derived from the sampling conditions of the 3DPXRT, see [2, 3]. Surprisingly, efficient sampling does not need any translation of the detector in this case: helical hexagonal interlaced scheme can be produced thanks to the QOD (Quarter Offset Detector). For fan beam helical tomography sampling, we need first to study the sampling condition of $\mathcal{D}_{e_3{}^\perp} f$.

1.2 Sampling and Shannon conditions

In the considered tomographic problem, we want to sample a function g being 2π-periodic in its first variable, π-periodic in its second variable and in $\mathbb{R}$ in its last variable. The Fourier transform

of $g \in C_0^\infty([0;2\pi[\times[0;\pi[\times\mathbb{R})$ can be defined by:

$$\hat{g}(\xi) = \frac{1}{2\pi^2\sqrt{2\pi}} \int_{[02\pi[} \int_{[0\pi[} \int_{\mathbb{R}} g(z) e^{-iz\cdot\xi}, dz$$

where $z = (\beta, \alpha, t) \in [0;2\pi[\times[0;\pi[\times\mathbb{R}$, $\xi = (k, m, \tau) \in \mathbb{Z} \times 2\mathbb{Z} \times \mathbb{R}$ and $\xi \cdot z = k\phi + m + \tau t$, see [4, 5]. The inverse Fourier transform defined for G a function on $\mathbb{Z} \times 2\mathbb{Z} \times \mathbb{R}$ is given by

$$\begin{aligned} \check{G}(z) &= (2\pi)^{-1/2} \int_{\mathbb{Z}\times 2\mathbb{Z}\times\mathbb{R}} G(\xi) e^{iz\cdot\xi} \\ &= (2\pi)^{-1/2} \sum_{k\in\mathbb{Z}} \sum_{m\in 2\mathbb{Z}} \int_{\tau\in\mathbb{R}} G(k,m,\tau) e^{i(k\beta+m\alpha+\tau t)} d\sigma. \end{aligned}$$

Let $\mathbf{K} \subset \mathbb{Z} \times 2\mathbb{Z} \times \mathbb{R}$, the non-overlapping Shannon condition associated to $\mathbf{K}$ for the sampling lattice $L_W = W\mathbb{Z}^3 \cap ([0;2\pi[\times[0;\pi[\times\mathbb{R})$ generated by the non singular 3×3 matrix W is that *the sets* $\mathbf{K} + 2\pi W^{-t} l, l \in \mathbb{Z}^3$ *are disjoint sets in* $\mathbb{Z} \times 2\mathbb{Z} \times \mathbb{R}$. The Petersen-Middleton theorem [10, 5] yields the Fourier interpolation formula

$$(S_W g)(z) = (2\pi)^{-1/2} |\det W| \sum_{y\in L_W} g(y) \check{\chi}_{\mathbf{K}}(z - y) \tag{4}$$

with the interpolation error

$$||S_W g - g||_\infty \leq 2(2\pi)^{-1/2} \int_{\xi\notin\mathbf{K}} |\hat{g}(\xi)| d\xi.$$

Thus if $\mathbf{K}$ is the essential support of $\hat{g}$, i.e., $\int_{\xi\notin\mathbf{K}} |\hat{g}(\xi)| d\xi$ can be negligible, then the interpolation error is low. The geometry of the set $\mathbf{K}$ can be exploited for the design of efficient sampling schemes, i.e., the choice of W satisfying the Shannon condition with $|\det W|$ maximal in oder to minimize the number of sampling points.

2 Essential support of the 3DFBXRT Fourier Transform

The main result of this paper is that, under the assumption that the function f is essentially b band limited (i.e., $\hat{f}(\xi)$ is negligible for $|\xi| > b$, $b > 0$, thus outside of the ball of radius b) the support of the 3DFBTRX Fourier transform is a bit larger than the set

$$K_{\mathcal{D}_{e_3}{}^\perp} = \{(k, m, \tau) \in \mathbb{Z} \times 2\mathbb{Z} \times \mathbb{R}; |k - m|^2 + r^2\tau^2 < r^2 b^2, |k|r < |k - m|\rho\}.$$

This results is a rather simple extension of the 2D fan beam sampling results by Natterer [7]. We give a sketch of the proof. From (3) we have

$$\begin{aligned} \hat{g}(k,m,\tau) &= \frac{1}{4\pi^2\sqrt{2\pi}} \int_{-\pi}^{\pi} \int_{-\pi}^{\pi} \int_{-\infty}^{\infty} \mathcal{P}f(\beta + \alpha - \pi/2, r\sin\alpha, t) e^{-i(k\beta+m\alpha+\tau t)} d\beta d\alpha dt \\ &= \frac{1}{4\pi^2} \int_{-\pi}^{\pi} \int_{-\pi}^{\pi} \widehat{\mathcal{P}f}^3(\beta + \alpha - \pi/2, r\sin\alpha, \tau) e^{-i(k\beta+m\alpha)}, d\beta d\alpha \end{aligned}$$

where $\widehat{\mathcal{P}f}^3$ is the monodimentional Fourier transform of $\mathcal{P}f$ according to its third variable. The projection slice theorem for the PXRT, see [6], yields

$$\widehat{\mathcal{P}f}(\beta + \alpha - \pi/2, \sigma, \tau) = \sqrt{2\pi}\hat{f}(\sigma\theta(\beta + \alpha - \pi/2) + \tau e_3).$$

Following [7] we obtain:

$$\begin{aligned} &\widehat{\mathcal{P}f}^3(\beta + \alpha - \pi/2, r\sin\alpha, \tau) \\ &= \frac{1}{\sqrt{2\pi}} \int_{\mathbb{R}} \widehat{\mathcal{P}f}(\beta + \alpha - \pi/2, \sigma, \tau) e^{i\sigma r\sin\alpha} d\sigma \\ &= \int_{\mathbb{R}} \hat{f}(\sigma\theta(\beta + \alpha - \pi/2) + \tau e_3) e^{i\sigma r\sin\alpha} d\sigma \\ &= \frac{1}{2\pi} \int_{\mathbb{R}^2} \hat{f}^3(x_1, x_2, \tau) \int_{\mathbb{R}} e^{-ix\cdot\theta(\beta+\alpha-\pi/2)+i\sigma r\sin\alpha} d\sigma dx_1 dx_2 \end{aligned}$$

As f is essentially b-band limited, the integral over $\sigma \in \mathbb{R}$ can be restricted to $|\sigma| < \sqrt{b^2 - \tau^2}$ (else $\hat{f}(\sigma\theta(\beta + \alpha - \pi/2) + \tau e_3)$ is negligible). This is the key point of the proof. From here, we can continue essentially the same proof as in [7] replacing the polar coordinates on x by cylinder coordinates and f by $\hat{f}^3$. This leads to the fact that $|\hat{g}(k, m, \tau)|$ decreases exponentially fast outside of the set $K_{\mathcal{D}_{e_3{}^\perp}}$.

3 Discussion

Clearly, from the shape of the set $K_{\mathcal{D}_{e_3{}^\perp}}$, we can construct efficient sampling schemes, such as interlaced and hexagonal-interlaced schemes, see [3] for similar 3D parallel schemes, see [7] in 2D. Adaptations to the helical constraint, as those given in [8] and [12] are simple and will be presented at the conference. However, the symmetry relation of the fan beam geometry $g(\beta, \alpha, t) = g(\beta + \pi + 2\alpha, -\alpha, t) = g\left((A(\beta, \alpha, t) + (\pi, 0, 0)\right)$, with A the 3×3 matrix $(1\ 2\ 0\ ;\ 0\ -1\ 0\ ;\ 0\ 0\ 1)$, and the shift $a = (\pi, 0, 0)$, can not be as simply handled as in parallel geometry. Indeed, see [9] and [11], the sampling of g on the lattice $\epsilon + Wk, k \in \mathbb{Z}^3$, where $\epsilon \in \mathbb{R}^3$ is a 3D shift, yields by the symmetry relation, the sampling on the lattice $AW\mathbb{Z}^3 + A\epsilon + a$. As the union of both lattices do not generally form a lattice, theorems like those in [1] are needed to exploit the symmetry of g. The stability of the schemes needs also to be studied.

References

[1] H. Behmard and A. Faridani. Sampling of band-limited functions on . *The Journal of Fourier Analysis and Applications*, 8:43–58, 2002.

[2] L. Desbat. Echantillonnage en tomographie 3D. In *Quinzième colloque sur le traitement du signal et des images, GRETSI'95*, pages 885–888, 1995.

[3] L. Desbat. Efficient sampling in 3D tomography: parallel schemes. In P. Grangeat and J.L. Amans, editors, *Three-Dimensional Image Reconstruction in Radiology and Nuc lear Medicine*, pages 87–100. Kluwer Academic, 1996.

[4] A. Faridani. An application of a multidimensional sampling theorem to computed tomography. In *AMS-IMS-SIAM Conference on Integral Geometry and Tomography*, volume 113, pages 65–80. Contemporary Mathematics, 1990.

[5] A. Faridani. A generalized sampling theorem for locally compact abelian groups. *Math. Comp.*, 63(207):307–327, 1994.

[6] F. Natterer. *The Mathematics of Computerized Tomography.* Wiley, 1986.

[7] F. Natterer. Sampling in fan-beam tomography. *SIAM J. Appl. Math.*, 53(2):358–380, 1993.

[8] F. Natterer. Resolution and reconstruction for a helical CT-scanner, 1996. Mathematics Dept., University Münster, Germany ; http://www.math.uni-muenster.de/math/inst/num/Preprints/1997/natterer_2/.

[9] F. Natterer. Sampling of functions with symmetries, 1999. Mathematics Dept., University Münster, Germany ; http://wwwmath.uni-muenster.de/math/inst/num/Preprints/1999/natterer_1/.

[10] D.P. Petersen and D. Middleton. Sampling and reconstruction of wavenumber-limited functions in N-dimensional euclidean space. *Inf. Control*, 5:279–323, 1962.

[11] P. La Rivière and X. Pan. Sampling and aliasing consequences of quarter detector ooset use in helical CT. *Preprint*, 2002.

[12] S. Roux, L. Desbat, A. Koenig, and P. Grangeat. Efficient acquisition protocole for cardiac dynamic CT. In *IEEE MIC conference record*, ., 2002.

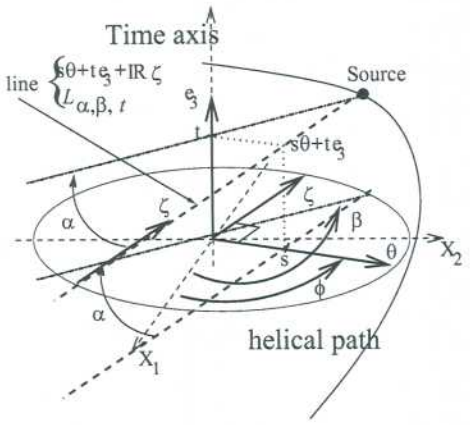

Figure 1: Geometrical parameters of the 3DFBXRT: All lines are perpendicular to the rotation axis direction e_3. Description of the parameters of the lines $L_{\beta,\alpha,t}$.

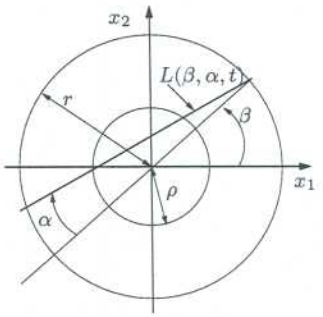

Figure 2: Parameters of the 3DFBXRT in the plane $x_3 = t$: r is the radius of the cylinder (source positions), r, β, t are the cylindrical coordinates of the source point, α is the angular position of the detector, ρ is the diameter of the cylinder containing the support of f.

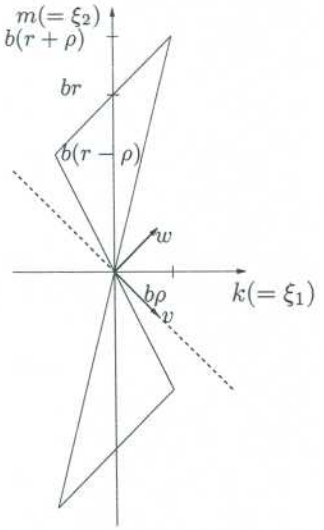

Figure 3: Representation of the set $K_{\mathcal{D}_{e_3}{}^{\perp}}$: slice $\tau = 0$ (i.e., the (k, m) plane),

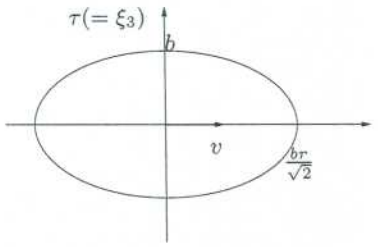

Figure 4: Representation of the set $K_{\mathcal{D}_{e_3}{}^{\perp}}$: slice $v = 0$ (i.e., the (u, τ) plane).

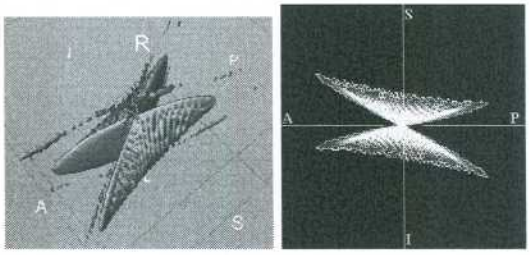

Figure 5: 3D Visualization of $K_{\mathcal{D}_{e_3}{}^{\perp}}$, essential support of $|\hat{g}(k, m, \tau)|$ obtained by computing the 3D Fourier transform of the 3DFBXRT of concentric ball indicators (simulating roughly a smooth peak). Bottom, visualization of $K_{\mathcal{D}_{e_3}{}^{\perp}}$ from the direction $-e_3$ (scales are modified because $g(\beta, \alpha, t)$ is sampled in α only within the fan-angle and not $[-\pi/2; \pi/2]$).